Synthesis and Microstructural Characterization of SnO$_2$:F Thin Films Deposited by AACVD

Karen Alejandra Chavarría-Castillo[a], Patricia Amézaga-Madrid[a]*, Oswaldo Esquivel-Pereyra[a],

Wilber Antúnez-Flores[a], Pedro Pizá Ruiz[a], Mario Miki-Yoshida[a]

[a] *Departamento de Física de Materiales, Centro de Investigación en Materiales Avanzados S.C., Miguel de Cervantes, No.120, C.P. 31136, Chihuahua, Chihuahua, México*

In this work, we report the synthesis and microstructural characterization of Tin oxide thin films doped with fluorine for applications such as transparent conductive oxides. Tin oxide doped with fluorine thin films were deposited by aerosol assisted chemical vapor deposition technique onto a borosilicate glass substrate, using a precursor solution of stannic chloride in ethanol and ammonium fluoride as the dopant. Deposition temperature was varied between 623-773 K. Also, other deposition parameters such as concentration of the precursor solution and gas carrier flux were fixed at 0.1 mol·dm^{-3} and 5 L min^{-1} respectively. Results indicate the presence of only the cassiterite phase of Tin oxide in all samples. Thin films obtained were characterized by X-Ray Diffraction. Surface morphology and microstructure were studied by field emission scanning electron microscopy, optical properties of samples were analyzed by total transmittance and reflectance spectra. The resistivity value of the films was measured by the sheet resistance.

Keywords: *Tin oxide films, SnO$_2$:F (FTO), Solar Cells, AACVD*

1. Introduction

Thin-film solar cells offer the opportunity to lower the price of solar energy by using small amount of nanomaterials and low-cost manufacturing technologies. A critical part of a thin-film solar cell however is the transparent electrode, which is commonly made of transparent conductive oxides (TCO), such as ITO (SnO$_2$-In), FTO (Fluor tin oxide, SnO$_2$-F) and ATO (SnO$_2$-Sb)[1-3]. Transparent conductive oxides (TCOs) have become increasingly important in a large variety of applications due to their wide variety of technological applications such as transparent electrodes in photovoltaic cells, gas sensors and many other opto-electronic devices [4]. However, the increasing demand and sophistication of active and passive devices based TCOs, results in the need to find new precursors and improve electrical and optical properties of synthesized materials. For practical use as transparent electrodes in devices such as solar cells, flat panel displays, and light emitting diodes, a TCO must have a resistivity of less than 10^{-3} Ω cm and over 80% transmittance in the visible range[5-7]. Indium tin oxide (ITO) is the current industrial standard material for transparent electrodes as thin films can be produced with resistivity in of the order of 10^{-5} Ω cm. However, due to the expense and scarcity of indium, alternatives need to be found. Among the available TCOs, SnO$_2$ seems to be more appropriate because they are quite stable toward atmospheric conditions, chemically inert, mechanically hard and can resist high temperature but its conductivity does not yet approach to that of the ITO[8]. Tin oxide (SnO$_2$) is a good candidate and a promising material

to improve its electrical and optical properties[9]. Its high reflectivity in infrared band makes it suitable for coatings on energy-saving windows. In order to use it as a conducting layer, the resistivity of SnO$_2$ has to be reduced. Therefore, fluorine (F) has been used as a dopant for SnO$_2$ where F substitutes the O^{-2} and acts as an electron donor, resulting in an n-type degenerate semiconductor[10]. Fluorine is an ideal substitution for oxygen because the anionic sizes are rather similar R$_O$$^{-2}$ =1.32Å and R$_F$ =1.33Å and the energy of dissociation (Do) of the Sn−F bond is similar to that of the Sn−O bond (~26.75 and ~31.05 Do/kJ mol^{-1} respectively)[11]. The use of fluorine doped tin dioxide for photovoltaics applications has risen from an almost zero market share in the year 2000 to a 50% share in 2009, with an impetus towards replacing sputtering deposition techniques with Chemical vapour deposition (CVD) [12]. Aerosol-assisted CVD (AACVD) is a variant of CVD. The main difference of this variant assisted by aerosol, is that transport of precursors to the synthesis zone is done in our case by using an ultrasonic nebulizer that has a piezoelectric vibrating at a frequency of 2.4 MHz which is responsible for the formation of a cloud of drops of micrometric average of 2.2 microns (aerosol) of the solution containing the element or elements of interest. For thin films, the substrate surface is first prepared by depositing therein a buffer layer of a metal oxide, and subsequently contacted with one or more precursors in vapor form that react or decompose to deposit the second nanostructured material desired. This aerosol was directed towards the substrate by a nozzle, which has a periodic movement at constant velocity to scan the whole surface of the substrate. This cloud of droplets is transported

* e-mail: patricia.amezaga@cimav.edu.mx

by a carrier gas, to a chamber temperature controlled, which is adhered on the substrate surface that forms the coating. The temperature of the chamber or substrate is one of the key parameters that control the production of the material. The precursor solution is also prepared easily and it is not necessary to control the pH, or use agents or additives to generate a particular morphology, it is only the precursor salt and solvent. Also, there is no necessity to apply heat treatments or subsequent washings to acquire a pure nanomaterial. The AACVD technique used in this work is simple, an attribute that makes it practical and versatile. A novelty of this method is that it is possible to obtain these pure materials in a single process, in the form of layers or multilayers of different materials without causing contamination of each other[13-15]. This process occurs at a lower cost, because in a continuous process, it does not require the use of special templates or additives agents to obtain a desired morphology in particular, allowing a uniform nanostructured materials deposit and allows to control of the dimensions of the thin films, depending of what is needed. This AACVD system is used to synthesize a convenient and relatively easy different nanomaterials with different morphologies as thin films in single layer or multilayers[14,17], nanorods and nanowires[16-19] nanorods coated[19] and hollow and mesoporous nanoparticles[20,21]. This technique, by its relative simplicity, can be easily manipulated and scalable industrially since it requires no high infrastructure or high vacuum systems, because it works at atmospheric pressure and therefore the above mentioned we can say that this process can occur at a lower investment.

This paper presents the synthesis by AACVD technique and characterization of thin films of pure tin oxide and tin oxide doped with fluorine at 5 at. % concentration in the precursor solution and synthesis temperatures (since 723-773 K), also, the influence of fluorine dopant in the structural, optical and electrical properties of the synthesized materials was analyzed.

2. Materials and methods

2.1 Synthesis

Undoped and F doped SnO_2 films were prepared onto TiO_2 thin film covered borosilicate glass substrates (2.5 × 7.5 cm^2) by the AACVD method details of the methodology were reported previously[16,22]. For TiO_2 layer deposition, the concentration of the starting solution was 0.05 mol·dm^{-3} of titanium (IV) oxyacetylacetonate (98%) in methanol (99.8%). For the SnO_2 thin films the precursor solution was of stannic chloride ($SnCl_4 5H_2O$) of 0.095 mol·dm^{-3} dissolved into ethanol (99.8%). For doped samples ammonium fluoride at 0.005 mol·dm^{-3} of concentration was utilized. The films were prepared at several temperatures: 623, 723, 748 and 773 K, and different deposition times. An ultrasonic nebulizer

(PG-241) working at 2.4 MHz generated the aerosol that was conveyed by the carrier gas and directed towards the substrate by a nozzle, which had a periodic movement at constant velocity (~1 cm.min^{-1}) to scan the whole surface of the substrate. Optimum parameters were determined and kept constant in all the samples reported in this work. The most important conditions were: temperature of 773 K, carrier gas (air) flow of 5 L min^{-1}, and distance from the nozzle to the substrate of 1 mm for all samples. The concentration of the precursor solution adjusted to 0.1 mol. L^{-1}. Table 1 summarizes the principal deposition parameters used in this work.

2.2. Characterization

Surface morphology and film's thickness were studied by field emission scanning electron microscopy (SEM) using a JEOL JSM-7401F operated at 5 kV. To determine the thickness, cross sectional samples of the films were observed. Elemental microanalysis of the films was achieved by energy dispersive X-ray spectroscopy (EDS), using an Inca microanalysis system attached to the electron microscope. Grazing incidence X-ray diffraction (GIXRD) patterns were acquired to determine the crystalline phases present in the films. The GIXRD patterns were obtained in a Pan-analytical X-Pert system, using Cu Kα radiation (λ = 0.1542 nm) at 40 keV and 35 mA. Grazing incidence angle was fixed at 0.5° and scanning angle 2 θ was varied between 25° and 90°, at 0.02° step. The optical properties of the materials were determined from total reflectance and transmittance measurements in the UV-VIS-NIR interval in a CARY 5000 spectrophotometer.

Resistivity was determined by the method of sheet resistance, for this measurement it was required: coating length (*l*) in m is the same in both directions and the sample thickness (*e*). Considering constant temperature, the resistance is given by the following expression (1):

$$R = \rho \frac{l}{s} = \rho \frac{l}{l \cdot e} \Rightarrow \rho = R \cdot e \quad (1)$$

Where ρ is the resistivity measured in Ω.m, *R* is the electrical resistance measured in Ω and *s* is the cross sectional area measured in m^2.

3. Results and Discussion

3.1. Structural properties

Films were polycrystalline, uniform, transparent and non-light scattering. Figure 1 (a-f) show SEM micrographs of surface morphology of samples. Figure 1 (a) shows the surface morphology of undoped sample A (SnO_2) prepared at 623 K and Figure 1 (b) shows the undoped sample B (SnO_2) prepared at 773 K. Samples A and B were prepared

Table 1: Temperature and time deposition, concentration of dopant fluorine in precursor solution, thickness of the samples, and also is presented commercial materials (TEC 8 and TEC 15) (produced by Pilkington NSG)[12,26]. Also is presented the resistivity value and percentage of transmittance obtained for each sample.

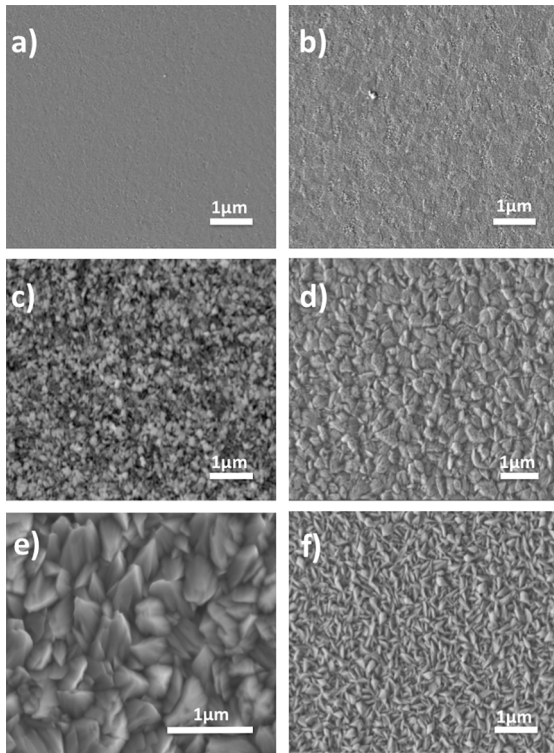| Sample	Ts [K]	Dopant F [at.% in solution]	Deposition time [min]	Deposition rate [nm min⁻¹]	Thickness [nm]	Resistivity [Ω • cm]	Transmittance [%]
A	623	0	15	6	90	1.17	84
B	773	0	15	7.33	110	9.88×10^{-1}	80
C	723	5	15	11.06	166	6.41×10^{-3}	70
D	748	5	20	12.55	251	6.05×10^{-3}	79
E	748	5	25	10.44	261	3.47×10^{-3}	76
F	773	5	30	10.56	317	3.17×10^{-3}	69
G	773	5	35	21.14	740	2.6×10^{-3}	70
TEC 8	873	-	-	-	650	5.2×10^{-4}	-
TEC 15	873	-	-	-	350	5.3×10^{-4}	-

Figure 1: (a-f). SEM images of the surface morphology of the all samples. a and b) Samples A and B, c-f) Doped samples (SnO₂:F) synthetized at different temperature and deposition time

as a reference, to be compared with doped samples. In both samples a flattened morphology is observed. A fine and uniform growth is appreciated in both samples (A and B) with a similar thickness of 90 and 110 nm respectively.

Figure 1 (c-f) shows the morphology of doped samples (SnO₂:F) (Samples C, D, F and G). It can be seen in Figure 1 (c-f) that doped samples show a significant change in morphology and also the formation of grains can be seen, these grains are uniformly distributed. In sample C (Figure 1c) we can see a morphology consisting of small grains with size of approximately 80-100 nm and with irregular shape; this sample has a thickness of 166 nm, and was synthetized at 723 K for a deposition time of 15 minutes. With increasing temperature (at 748 K), and the deposition time (20 minutes) another change is seen in the morphology, (sample D, Figure 1 d), resulting grains with a size of 250-500 nm and a thickness of 251 nm. Furthermore, samples F and G were synthetized at the same temperature (773 K) and only deposition time 30 to 35 minutes respectively was varied. We can see that in Figure 1e (sample F) reoccurring grain growth having a grain size of 200-500 nm, similar in shape to sample D, and obtaining a thickness of 317 nm. However, Sample G shows the opposite behavior, the grain size decreases but retains its irregular shape, and the thickness increases to 740 nm. The difference between these two samples is the deposition time to be increased from 30 to 35 minutes. The morphologies obtained in this study are similar to those reported in[27]. In short, we can say with these results that the presence of dopant fluorine and the amount that goes into each sample has an important influence in changing the microstructure of the samples and grain sizes, to analyze the values in the rate deposition in the samples (see Table 1), it is observed that the values are very close, there is no significant difference between them, which means that the deposition temperature and the deposition time, do not exert significant influence in changing the morphology of the samples. Similar results of SnO₂:F were reported in [1]. In the case of EDS analysis, in the samples A and B the presence of the next elements is noted: Sn % at. of 0.56 and 1.82; O % at. of 68.13 and 68.56; Si % at. 27.07 and 25.71 (substrate element); Na % at. of 1.88 and 1.35 (substrate element); Al % at. of 1.12 and 0.88 (substrate element); Ti % at. of 1.25 and 1.68 (substrate element and the barrier layer) respectively, all elements measured at the level K. In the case of doped samples exhibit similar % at. of the elements present that in the sample B (reported above), however the element F was not detected, this can be explained because there was possibly a minor amount of dopant that could not be detected by the analyzer.

The crystal structure of the deposited doped and undoped thin films was determined by X-ray diffraction technique. According to GIXRD patterns in Figure 2 (pure SnO_2 samples A and B) and Figure 3 (SnO_2:F samples F and G), it was concluded that all samples were polycrystalline. A representative peak of TiO_2 as anatase (barrier layer) was observed at 25.23° (PDF 01-075-2553)[23]. And the figures 2 and 3 show clearly that it only contains crystal lattice planes of (110), (101), (200), (211), (220), (310), (301) matched with diffracting lines of SnO_2 as tetragonal cassiterite (PDF 01-072-1147)[24].
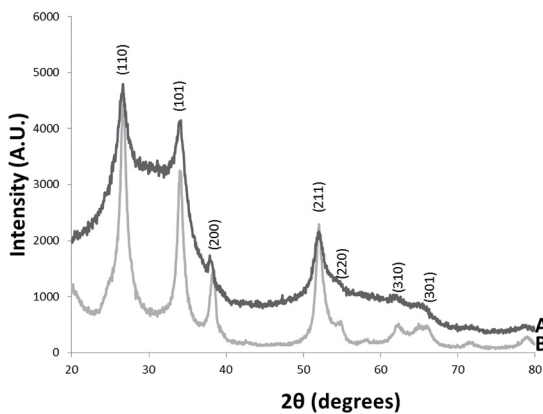

Figure 2: GIXRD patterns of SnO_2 samples (A and B).
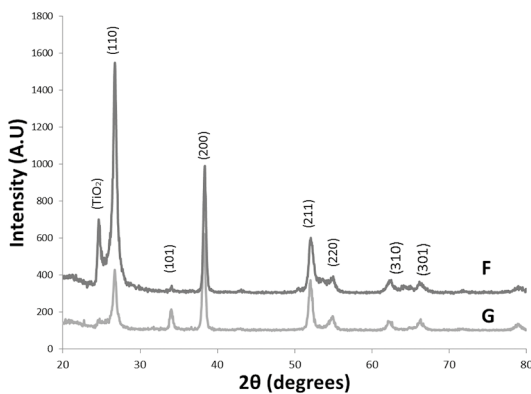

Figure 3: GIXRD patterns of doped samples with fluorine. (Samples F and G). These samples presented only single-phase cassiterite structure.

3.2. Optical and electrical properties

All samples had a similar behavior in the visible region. Figure 4 shows the transmittance (T) spectra of sample A (pure SnO_2) and samples F and G (SnO_2:F). High transparency in the visible range (60-80%) is observed, in the wavelength range 450-850 nm, in accordance with the requirements for transparent conducting oxide applications (80%),[9,25] indicating that doping does not affect the properties of the material. Doped SnO_2 films showed n-type conductivity.
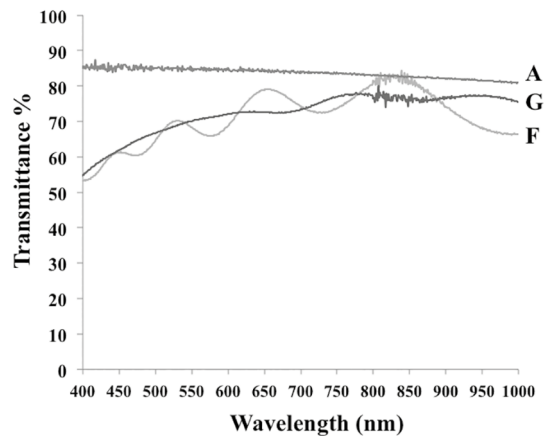

Figure 4: Transmittance spectra obtained of the A, G and F samples

Table 1 displays the resistivity values; as it can be seen, the doped films are all conductive, this is because the doping with fluorine. All doped samples, showed a good resistivity values in the order of 10^{-3} Ω · cm, since smaller thicknesses (166 nm) (sample C) using low temperatures (723-773 K) and short times of deposition (15-30 minutes) is achieved, resistivity decrease two orders of magnitude (comparing with sample B) managing to obtain resistivity of the order of magnitude of 10^{-3} Ω · cm. There are already commercial products with resistivity on the order 10^{-4} Ω · cm, In Table 1, two commercial materials (TEC 8 and TEC 15) produced by the company Pilkington NSG[12,26] are presented, these commercial materials are glass with a coating of FTO that are deposited by means of physical-chemical processes (using chemical vapor) and / or physical (high vacuum) at temperatures of 873 K [26] these results give us the opportunity to continue working to improve the conductive property of our materials using techniques such as AACVD.

4. Conclusions

Undoped and fluorine doped tin oxide films with high quality were successfully deposited using a simplified and inexpensive AACVD technique for electrical applications. The structural, morphological, optical and electrical properties were investigated as a function of deposition temperature (723-773 K), different deposition times and 5 % at of dopant F in solution. All doped samples, showed a good resistivity values in the order of 10^{-3} Ω · cm since 723 K and 166 nm of thickness. SnO_2:F with 740 nm of thickness exhibited the lowest resistivity around 2.6×10^{-3} Ω · cm. High transparency in the visible range (60-80%) is observed in all doped samples, in the wavelength range 450-850 nm, in accordance with the requirements for transparent conducting oxide applications. These nanomaterials obtained by this technique are promising materials for use due to their production at lower cost. Coated glass demand grows with

the development of the industry of solar power generation, so it is necessary to opt for synthesis techniques with lower cost and infrastructure.

5. Acknowledgement

6. References

1. Supriyono, Surahman H, Krisnandi YK, Gunlazuardi J. Preparation and characterization of transparent conductive SnO$_2$-F thin film deposited by spray pyrolysis: relationship between loading level and some physical properties. *Procedia Environmental Sciences*. 2015;28:242-251.

2. Moholkar AV, Pawar SM, Rajpure KY, Bhosale CH, Kim JH. Effect of fluorine doping on highly transparent conductive spray deposited nanocrystalline tin oxide thin films. *Applied Surface Science*. 2009;255(23):9358-9364.

3. Olopade MA, Awe OE, Awobode AM, Alu N. Characterization of SnO$_2$:F films deposited by atmospheric pressure chemical vapor deposition for optimum performance solar cells. *The African Review of Physics*. 2012;7:177-181.

4. Fukano T, Motohiro T. Low-temperature growth of highly crystallized transparent conductive fluorine-doped tin oxide films by intermittent spray pyrolysis deposition. *Solar Energy Materials and Solar Cells*. 2004;82(4):567-575.

5. Brabec CJ, Cravino A, Meissner D, Sariciftci NS, Fromherz T, Rispens MT, et al. Origin of the Open Circuit Voltage of Plastic Solar Cells. *Advanced Functional Materials*. 2011;11(5):374-380.

6. Too CO, Wallace GG, Burrell AK, Collis GE, Officer DL, Boge EW, et al. Photovoltaic devices based on polythiophenes and substituted polythiophenes. *Synthetic Metals*. 2001;123(1):53-60.

7. Goetzberger A, Hebling C, Schock HW. Photovoltaic materials, history, status and outlook. *Materials Science and Engineering: R: Reports*. 2003;40(1):1-46.

8. Gupta S, Yadav BC, Dwivedi P, Das B. Microstructural, optical and electrical investigation of Sb-SnO$_2$ thin films deposited by spray pyrolysis. *Materials Research Bulletin*. 2013;48(9):3315-3322.

9. Abhijit AA, Pawar SC, Patil DH, Ghogare MD. Properties of (200) oriented, highly conductive SnO$_2$ thin films by chemical spray pyrolysis from non-aqueous medium: Effect of antimony doping. *Journal of Alloys and Compounds*. 2015;652:145-152.

10. Miki-Yoshida M, Andrade E. Growth and structure of tin dioxide thin films obtained by an improved spray pyrolisis technique. *Thin Solid Films*. 1993;224(1):87-96.

11. Ngamsinlapasathiana S, Sreethawongb T, Suzuki Y, Yoshikawa S. Doubled layered ITO/SnO$_2$ conducting glass for substrate of dye-sensitized solar cells. *Solar Energy Materials and Solar Cells*. 2006;90(14):2129-2140.

12. Bachu DS, Waugh MR, Zeissler K, Branford WR, Parkin IP. Textured Fluorine-Doped Tin Dioxide Films formed by Chemical Vapour Deposition. *Chemistry - A European Journal*. 2011;17(41):11613-11621.

13. Sáenz-Trevizo A, Amézaga-Madrid P, Pizá-Ruiz P, Solís-Canto O, Ornelas-Gutiérrez C, Pérez-García A, et al. Microstructural characterization, optical and photocatalytic properties of bilayered CuO and ZnO based thin films. *Journal of Alloys and Compounds*. 2014;615(Suppl 1):S375-S381.

14. Sáenz-Trevizo A, Amézaga-Madrid P, Fuentes-Cobas L, Pizá-Ruiz P, Ornelas-Gutiérrez C, Pérez-García A, et al. Microstructural, chemical and textural characterization of ZnO nanorods synthesized by aerosol assisted chemical vapor deposition *Materials Characterization*. 2014;98:215-221.

15. Sáenz-Trevizo A, Amézaga-Madrid P, Pizá-Ruiz P, Antúnez-Flores W, Ornelas-Gutiérrez C, Miki-Yoshida M. Efficient and durable ZnO core-shell structures for photocatalytic applications in aqueous media. *Materials Science in Semiconductor Processing*. 2016;45:57-68.

16. Miki-Yoshida M, Patricia Amézaga-Madrid P, Pizá-Ruiz P, Antúnez-Flores W, Lugo-Ruelas M, Esquivel-Pereyra O, inventors. *Application for patent registered with the Mexican Institute of Industrial Property*. Document number MX/a/2013/015380; folio MX/E/2013/095195.

17. Lugo-Ruelas M, Amézaga-Madrid P, Esquivel-Pereyra O, Antúnez-Flores W, Pizá-Ruiz P, Ornelas-Gutiérrez C, et al. Synthesis, microstructural characterization and optical properties of CuO nanorods and nanowires obtained by aerosol assisted CVD. *Journal of Alloys and Compounds*. 2015;643(Suppl 1):S46-S50.

18. Amézaga-Madrid P, Antúnez-Flores W, González-Hernández J, Sáenz-Hernández J, Campos-Venegas K, Solís-Canto O, et al. Microstructural properties of multi-nano-layered YSZ thin films. *Journal of Alloys and Compounds*. 2010;495(2):629-633.

19. Miki-Yoshida M, Amézaga-Madrid P, Sáenz-Trevizo A, Pizá-Ruiz P, Antúnez- Flores W, Lugo-Ruelas M, inventors. Centro de Investigación en Materiales Avanzados, S.C. México. Patent register MX/a/2014/007867.

20. Monárrez-Cordero B, Amézaga-Madrid P, Antúnez-Flores W, Leyva-Porras C, Pizá-Ruiz P, Miki-Yoshida M. Highly efficient removal of arsenic metal ions with high superficial area hollow magnetite nanoparticles synthetized by AACVD Method. *Journal of Alloys and Compounds*. 2014;586(Suppl 1):S520-S525.

21. Miki-Yoshida M, Amézaga-Madrid P, Monárrez-Cordero BE, Barrientos-Juárez E, inventors. Centro de Investigación en Materiales Avanzados, S.C. México. Title of Patent No. MX/a/2012/004874.

22. Amézaga-Madrid P, Antúnez-Flores W, Monárrez-García I, González-Hernández J, Martínez-Sánchez R, Miki-Yoshida M. Synthesis, structural characterization and optical properties of multilayered Yttria-stabilized ZrO$_2$ thin films obtained by aerosol assisted chemical vapour deposition. *Thin Solid Films*. 2008;516(23):8282-8288.

23. International Center for Diffraction Data. *ICDD XRD database PDF number 01-075-2553*. Newtown Square: International Center for Diffraction Data; 1990.

24. International Center for Diffraction Data. *ICDD XRD database PDF number 01-072-1147*. Newtown Square: International Center for Diffraction Data; 1990.

25. Guillén C, Herrero J. TCO/metal/TCO structures for energy and flexible electronics. *Thin Solid Films*. 2011;520(1):1-17.

26. Pilkington NSG Group Flat Glass Business. *NSG TEC™*. Available from: <https://www.pilkington.com/en-gb/uk/products/product-categories/solar-energy/nsg-tec>. Access in: 10/10/2016.

27. Noor N, Parkin IP. Enhanced transparent-conducting fluorine-doped tin oxide films formed by Aerosol-Assisted Chemical Vapour Deposition. *Journal of Materials Chemistry C*. 2013;1(5):984-996.